A MORE REDUCED MANTLE SOURCE FOR ENRICHED SHERGOTTITES; INSIGHTS FROM OLIVINE-PHYRIC SHERGOTTITE LAR 06319. A. H. Peslier[1,2], D. Hnatyshin[3], C.D.K. Herd[3], E.L. Walton[4], A.D. Brandon[5], T.J. Lapen[5] and J. Shafer[5], [1]Jacobs Technology, E.S.C.G., Mail Code JE23, 2224 Bay Area Blvd, Houston, TX 77058, USA, anne.h.peslier@nasa.gov, [2]ARES, NASA-Johnson Space Center, Houston, TX 77058, USA, [3]Earth & Atmospheric Sciences, University of Alberta, Edmonton, Alberta T6G 2E3, Canada, [4]Physical Sciences, Grant MacEwan University, City Center Campus, Edmonton, Alberta, T5J 2P2, Canada, [5]Earth and Atmospheric Sciences, University of Houston, Houston, TX 77204-5007, USA.

Summary: A detailed petrographic study of melt inclusions and Cr-Fe-Ti oxides of LAR 06319 leads to two main conclusions: 1) this enriched oxidized olivine-phyric shergottite represents nearly continuous crystallization of a basaltic shergottite melt, 2) the melt became more oxidized during differentiation. The first crystallized mineral assemblages record the oxygen fugacity which is closest to that of the melt's mantle source, and which is lower than generally attributed to the enriched shergottite group.

Introdution: Shergottites span a wide range of oxygen fugacities, trace element, and radiogenic isotope characteristics and are traditionally split into 3 groups (Fig. 1). The 'depleted reduced' group has lower oxygen fugacity (log units relative to the fayalite-magnetite-quartz buffer FMQ -4 to -2), chondrite-normalized light rare earth element (LREE) depleted patterns, and low $^{87}Sr/^{86}Sr$ and high $\varepsilon^{143}Nd$. The 'enriched oxidized' group has higher oxygen fugacity (FMQ -1.5 to 0.5), flat REE patterns, and high $^{87}Sr/^{86}Sr$ and low $\varepsilon^{142}Nd$. The third group is intermediary. LAR 06319 was found in the Larkman Nunataks range of Antarctica in 2006. It is composed of large olivine megacrysts (Fo_{76-50}) containing melt inclusions, large zoned pyroxenes (pigeonite and augite), and Cr-spinels set in a matrix of maskelynite, Fe-rich pyroxenes, Fe-Ti oxides, sulfides, phosphates, Si-rich glass, and baddeleyite. LAR 06319 is an olivine-phyric shergottite, and belongs to the enriched oxidized shergottite group (*1, 2*).

Methods: Two rock sections were analyzed by electron microprobe at NASA-JSC (Cameca SX100) and at the University of Alberta (JEOL JXA8900). Detailed spot analyses and elemental maps were acquired for the melt inclusions and Cr-Fe-Ti oxides.

Melt inclusions: Olivine megacrysts with Fo_{76-60} contain large (250 x 100 μm) silicate inclusions made of various minerals and glasses. These inclusions have a roughly concentric arrangement of phases with, from edge to center, a thin (<10 μm) layer of Ca-poor pyroxene, a thicker layer (10-15 μm) of Ca-rich (CaO = 20 wt %) pyroxene, and a center made of more Ca-poor pyroxene mixed with Si-rich glass (71-93 wt % SiO_2). Inclusions of crystallized melt trapped in olivine phenocrysts may potentially record the magmatic pre-eruptive conditions (*3*). Olivine is generally the first mineral on the liquidus and trapped melt inclusions should represent the state of the magma before it evolved significantly through differentiation, degassing, oxidation and assimilation of the rocks traversed during the magma's rise to the planet's surface. The various phases forming the inclusions in the olivine megacrysts result from closed-system crystallization during slow cooling after the melt was trapped in the olivine (*3, 4*).

The compositions of the various phases found in the LAR 06319 olivine inclusions and the electron microprobe element maps of the inclusions were used to estimate the relative abundance of these phases, reconstitute a bulk composition of the inclusion, and recalculate the inclusion compositions before Fe-Mg exchange with their olivine host (*5*). The obtained bulk compositions of the melt inclusions located in the most Mg-rich part of the olivine megacrysts resemble parent melts and whole rock compositions of basaltic shergottites (*6-8*). These melt inclusion compositions were used as parent melts in the MELTS software (9-10) to reproduce the crystallization sequence of LAR 06319. Both petrographic observations and the fact that the melt inclusion compositions appear to represent parent melts can be used to conclude that LAR 06319 represents near continuous differentiation of a basaltic shergottitic melt.

Cr-Fe-Ti oxides: LAR 06319 contains 6 types of oxides. Type 1 is one of the earliest phase crystallized and is a Cr-spinel. Type 2 and 3 are ülvospinels. Type 4 and 5 (ilmenites), and Type 6 (magnetite) are later stage phases.

Oxygen fugacity: The assemblages in LAR 06319 are conducive to the application of oxybarometers, and our results allow us to elucidate the oxygen fugacity-temperature history of the rock. Detailed oxybarometry was conducted on olivine-pyroxene-spinel ((*11*), (*12*), and Computational Thermodynamic Server of Sacks and Ghiorso) and ilmenite-magnetite ((*13*), and Ca-QUIlF models of (*14*)) assemblages. In addition, we used our own method of correction for Fe-Mg exchange between spinel and host or adjacent minerals.

The earliest phases in LAR 06319 are represented by megacrystic olivine, Mg-rich pyroxene cores, and T1 spinels. They formed from a melt with an oxygen fugacity of around FMQ – 2. As the melt cooled the crystallizing olivine and pyroxene became more Fe-rich and co-crystallized with T2 spinel. During this phase oxygen fugacity varies from FMQ – 0.9 to ~ FMQ with increasing Ti content and decreasing Cr content of the spinel. All later crystallization products - T3 and T6 spinel and T4 and T5 ilmenite – crystallized within 0.5 log units of FMQ, consistent with the presence of almost pure SiO_2. The change from FMQ – 2 to FMQ – 0.9 is the only significant jump in oxygen fugacity and is relatively small. Oxygen fugacity can consequently vary by two log units during closed-system crystallization of a basaltic melt.

Conclusion: Only the first phases to crystallize in LAR 06319, at FMQ -2, likely record the oxidation conditions closest to those of the mantle reservoir from which the parent melt was derived. FMQ -2 is below the lower end of the typical range (FMQ -1.5 to 0.5) for the oxidized shergottite group. The more oxidized values recorded by other enriched shergottites may thus record mainly processes of fractionation with only the most oxidized phase assemblages left for us to examine: processes such as fractional crystallization and removal of reduced phases, assimilation of oxidized or hydrous material, degassing, and decompression during magma ascent may increase oxygen fugacity values (*11, 15-17*). LAR 06319 offers the opportunity to obtain the best estimate of the oxygen fugacity of the enriched shergottite reservoir, i.e. FMQ -2 ±0.5. The narrower range (FMQ -4 to -2) than previously thought (FMQ -4 to 0.5) of oxygen fugacities for the martian mantle, may be now easier to explain by a process such as planet-wide slow crystallization and stratification.

References:

[1]A. B. Sarbadhikari, J. M. D. Day, Y.-G. Liu, D. Rumble III, L. A. Taylor (2009) *GCA* 73, 2190.

[2] A. H. Peslier, D. Hnatyshin, C.D.K. Herd, E.L. Walton, A.D. Brandon, T.J. Lapen, J. Shafer (2010) *GCA* submitted.

[3] A. J. R. Kent (2008) in *Minerals, inclusions and volcanic processes,* K. D. Purtika, F. J. Tepley III, Eds. (Min. Soc. America, Chantilly, VA) vol. 69, 273-331.

[4] E. Roedder (1979) *Bull. Min.* 102, 487.

[5] L. V. Danyushevsky (2001) *JVGR* 110, 265-280.

[6] J. Longhi, V. Pan (1989) *19th LPSC* Houston, TX, 451-464.

[7] K. Lodders (1998) *Meteor. Planet. Sci.* 33, A183.

[8] J. C. Bridges, P. H. Warren (2006) *J. Geol. Soc. London* 163, 229-251.

[9] M. Ghiorso, R.O. Sack (1995) *CMP* 119, 197-212

[10] P.D. Asimow, M.S. Ghiorso (1998) *Am. Min.* 83, 1127-1132

[11] C. D. K. Herd, L. E. Borg, J. H. Jones, J. J. Papike (2002) *GCA* 66, 2025-2036.

[12] B. J. Wood (1991) in *Oxide minerals: petrologic and magnetic significance,* D. H. Lindsley, Ed. (Min. Soc. America), vol. 25, 417-431.

[13] M. S. Ghiorso, B. W. Evans (2008) *AJS.* 308, 957-1039.

[14] D. J. Andersen, D. H. Lindsley, P. M. Davidson (1993) *CG* 19, 1333-1350.

[15] C. A. Goodrich, C. D. K. Herd, L. A. Taylor (2003) *MAPS* 38, 1773-1792.

[16] C. D. K. Herd (2006) *AM.* 91, 1616-1627.

[17] C. Ballhaus, B. R. Frost (1994) *GCA* 58, 4931.

[18] C. D. K. Herd, J. J. Papike, A. J. Brearley(2001) *AM* 86, 1015-1024.

[19] C. D. K. Herd (2003) *MAPS* 38, 1793-1805.

[20] C. Meyer (2009) (ARES), vol. JSC #27672 Revision C.

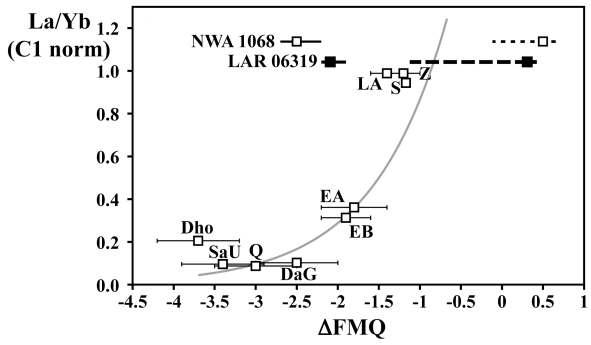

Fig. 1: C1 chondrite normalized whole rock La/Yb ratio versus oxygen fugacity for LAR 06319 and a selection of shergottites. Oxygen fugacity data are from the following sources: (*18*) for Shergotty (S), Zagami (Z), Los Angeles (LA), EET 79001 Lithology B (EB), and QUE 94201 (Q); (*19*) for EET 79001 Lithology A (EA), Dar al Gani 476 (DaG), Sayh al Uhaymir 005 (SaU), and Dhofar 019 (Dho); (*16*) for NWA 1068. For both NWA 1068 and LAR 06319, two data points are given: estimates from the earliest assemblages at lower oxygen fugacity and estimates for latest (groundmass) assemblages at higher oxygen fugacity; the range of oxygen fugacity during crystallization in each meteorite is shown by solid and dashed lines. For NWA 1068, the La/Yb ratio of the whole rock is utilized for plotting both oxygen fugacity estimates. For LAR 06319, the whole rock La/Yb ratio is used to plot the groundmass oxygen fugacity, whereas the melt inclusion La/Yb ratio is used to plot the megacryst oxyen fugacity. REE data are from various sources in (*20*), and (*1*). The polynomial line-of-best-fit (grey line) does not include data from NWA 1068 or LAR 06319.